

Southern African Large Telescope



Title: **RSS: Radial Velocity Accuracy using Emission Lines**

Author(s): **Alexei Kniazev**

Doc. number: **2202AA0001**

Version: **1.1**

Date: *July 23, 2012*

Keywords: RSS, velocities, emission lines

Approved: **David Buckley (Ast Ops Manager)**

Signature: _____ Date: _____

ABSTRACT

I present my study of the accuracy of radial velocity measurements for spectral data taken with RSS. This study is only done for the case of objects with emission lines. Data for gratings GR900 and GR1800 were analysed. I describe in detail the procedure for measurement and obtaining of the results. All analysed data showed that with SALT/RSS data user can routinely reach an accuracy of $\sim 10 \text{ km s}^{-1}$ with grating GR900 and $\sim 5 \text{ km s}^{-1}$ with grating GR1800. No systematic shifts were detected.



Contents

1	Introduction	4
2	Data	4
2.1	Taken Data	4
2.2	Data Reduction	4
2.3	Data Analysis	5
3	Results	9
3.1	Data with grating VPH1800	9
3.1.1	Data for the dust-lane polar-ring galaxy AM 1934-563	9
3.1.2	Data for the dwarf irregular galaxy IC 4662	9
3.2	Data with grating VPH900	11
3.2.1	Data for lenticular galaxies	11
3.2.2	Velocities for PNe in the CMa region	11
4	Conclusions	13

List of Figures

1	Emission $H\alpha$ line along the slit for the galaxy NGC 216. <i>Top panel:</i> Distribution of emission line intensity (red), background around of this line (black) and noise (blue). <i>Middle panel:</i> Intensity contour map of the 2D $H\alpha$ spectrum with line centers overplotted in red. <i>Bottom panel:</i> The final Position–Velocity diagram along the slit. For each point 1σ error is shown. The green line shows the region along the slit which was used to estimate weighted mean for the velocity. The Y-position of the green line shows the value of the weighted mean velocity.	6
2	<i>Top panel:</i> The solid line shows the profile of the $H\alpha$ flux along the major axis, after the continuum subtraction. The dotted line shows the continuum intensity distribution along the slit and in the spectral region of the $H\alpha$ line. <i>Middle panel:</i> Radial velocity distribution along the major axis of AM 1934-563. The black squares, red squares and blue triangles represent measurements of the emission lines $H\alpha$, $[N\ II]\ \lambda 6583$ and $[S\ II]\ \lambda 6716$ respectively. The black filled circles show the stellar velocity distribution measured from the absorption doublet $Na\ I\ D\ \lambda\lambda 5890, 5896$. One σ error bars have been overplotted for all measurements. The solid blue line is the result of a linear fit to all measurements of the $Na\ I\ D$ lines. <i>Bottom panel:</i> The measured FWHM of the $H\alpha$ line, corrected for the intrinsic line width of the RSS. The FWHM of the reference night-sky line measured in each row is shown with open squares.	7



- 3 The galacto-centric velocity distributions along the major axis of AM 1934-563. The small black filled circles red squares are for the NW branch using the emission lines of $H\alpha$ and $[N II] \lambda 6583$ lines, respectively. The blue and green filled circles stand for the SE branch using the $H\alpha$ and $[N II] \lambda 6583$ lines. The larger filled black circles show the stellar velocity distribution measured from the absorption doublet $Na I D \lambda\lambda 5890, 5896$. The solid blue line is the result of a linear fit to all measurements for the $Na I D$ lines. Big black filled lozenges and triangles inside squares represent the Reshetnikov et al. (2006) data for $H\alpha$ and $[N II] \lambda 6583$, respectively. These values have not been corrected back for cosmological stretch. 8
- 4 *Top figure:* RSS data. The solid line in the upper panel shows the profile of the $H\alpha$ flux along the major axis, after the continuum subtraction. Radial velocity distribution along the major axis of IC 4662 is shown in the bottom panel with 1σ errors for each point. *Bottom figure:* Radial velocity distribution along the major axis of IC 4662 from Figure 12 of van Eymeren et al. (2010): Optical data are shown with symbols '+'. HI velocities are shown with a solid line. . . 10
- 5 The comparison between SALT and other measurements. Each point is shown with 1σ error. Errors for SALT data are shown with red colour and errors from Schneider et al. (1983); Durand, Acker & Zijlstra (1998) are shown with green colour. Black lines shows the equality relation. 12



1 Introduction

Understanding the accuracy of velocities measurements is vital for the proposal preparation procedure. Currently the SALT database has enough RSS data to estimate this accuracy for different RSS gratings. In this report I analyse some data in order to show the accuracy of RSS data obtained in the standard way.

The method described below was used by the author previously to analyse data taken with different telescopes and instrumentation: long-slit spectrograph with 6-m SAO RAS telescope, TWIN with 3.5m at Calar Alto, EMMI with NTT ESO, CAFOS with 2.2m at Calar Alto. In all cases small shifts exist after wavelength calibrations (possibly due to flexure) and were needed to be corrected finally during the analysis.

2 Data

2.1 Taken Data

Observational data were taken with RSS during 2006–2012. All data were extracted from SALT database. All used data are shown in Table 1. In my study I used spectral data taken with the Volume Phase Holographic (VPH) gratings GR900 and GR1800, since both of them are often used for extragalactic studies, where emission lines are very often used for different scientific needs. All analysed observations were taken with a binning factor of 2 x 2. Grating GR900 has a final reciprocal dispersion of $\sim 0.97 \text{ \AA pixel}^{-1}$ and a spectral resolution FWHM of 4–5 \AA for slits 1.25–1.5 arcsec. VPH grating GR1800 has a final reciprocal dispersion of $\sim 0.41 \text{ \AA pixel}^{-1}$ and a spectral resolution FWHM of 2–2.5 \AA for slits 1.5–2.0 arcsec.

RSS data were taken in blocks, where each block consist of some science frames with the same spectral setup and reference spectrum observed thereafter. After each block the spectral setup of RSS was changed. For this reason we have to conclude that each block is independent, and we can compare data from different blocks as independent data. The accuracy for the measured velocities in each block is limited by several factors:

- (1) 2D wavelength calibration
- (2) known RSS flexure
- (3) possible other systematic and random effects.

2.2 Data Reduction

Primary data reduction was done with the SALT science pipeline described in Crawford et al. (2010). Subsequent data reduction was done as described in Kniazev et al. (2008).

The derived internal errors for the 2D wavelength calibrations do not exceed 0.3 \AA for grating GR900 or $\leq 15 \text{ km s}^{-1}$ for the spectral region of H α line ($\lambda 6562 \text{ \AA}$). Usually, the derived internal error for the 2D wavelength calibration for grating GR900 is about 0.2 \AA ($\sim 1/5$ of the reciprocal dispersion) or $\sim 10 \text{ km s}^{-1}$.

For grating GR1800 the derived internal errors for the 2D wavelength calibrations do not



Table 1: Analysed observations

Date	Slit	Binning	Grism	Comment
20.09.2006	1.5	2×2	GR1800	AM 1934-563
31.05.2006	1.5	2×2	GR1800	IC 4662
16.05.2011	1.0	2×2	GR900	lenticular galaxies
09.09.2011	1.0	2×2	GR900	lenticular galaxies
15.01.2012	1.25	2×2	GR900	PNe in CMa
16.01.2012	1.25	2×2	GR900	PNe in CMa
18.01.2012	1.25	2×2	GR900	PNe in CMa
27.01.2012	1.25	2×2	GR900	PNe in CMa
28.01.2012	1.25	2×2	GR900	PNe in CMa
29.01.2012	1.25	2×2	GR900	PNe in CMa
30.01.2012	1.25	2×2	GR900	PNe in CMa

exceed 0.2 \AA or $\leq 10 \text{ km s}^{-1}$ for the spectral region of $\text{H}\alpha$ line. Usually, the derived internal error for grating GR1800 is about 0.08 \AA ($\sim 1/5$ of the reciprocal dispersion) or $\sim 4 \text{ km s}^{-1}$.

2.3 Data Analysis

To exclude systematic shifts originating from possible RSS flexure and other systematic and random effects, we calculated the line-of-sight velocity distributions along the slit using the method described in Zasov et al. (2008). The procedure includes the following steps:

- (1) a measurement of the position of the studied emission line for each row, using gaussian fitting;
- (2) an estimation of the background and the S/N ratio for the emission line in each row;
- (3) a similar measurement of the nearby night-sky line in the 2D wavelength calibrated spectrum and compiling the table of differences between the laboratory wavelength of this line and the measured one for each row;
- (4) polynomial fitting of these differences and a determination of the residual scattering (r.m.s.);
- (5) the application of this fitting polynomial in order to correct the measured wavelengths of the studied emission line. The resulting error of wavelengths measurements is determined by the quadratic summing of the fitting r.m.s., found in the previous step, and the measurement error of velocity for each point along a slit, estimated from gaussian fitting;

All velocities derived with this procedure are heliocentric. All programs were created using MIDAS command language. An example of the procedure output is shown in Figure 1.

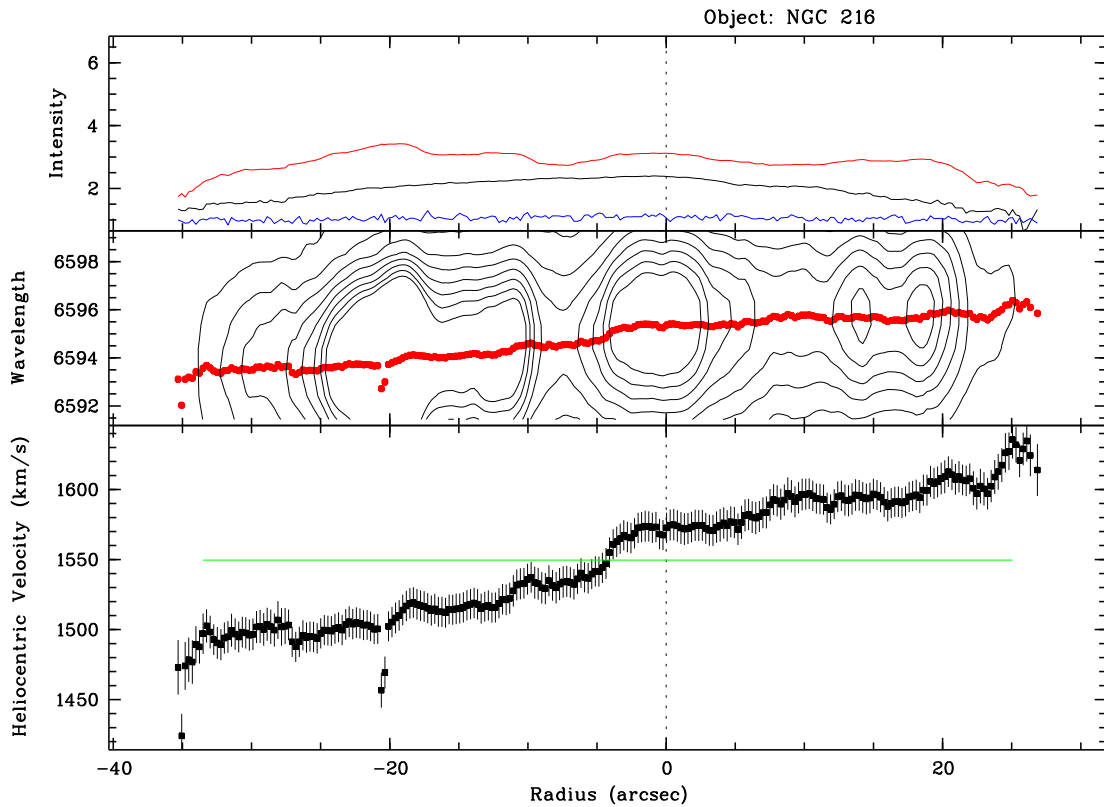


Figure 1: Emission $H\alpha$ line along the slit for the galaxy NGC 216. *Top panel:* Distribution of emission line intensity (red), background around of this line (black) and noise (blue). *Middle panel:* Intensity contour map of the 2D $H\alpha$ spectrum with line centers overplotted in red. *Bottom panel:* The final Position–Velocity diagram along the slit. For each point 1σ error is shown. The green line shows the region along the slit which was used to estimate weighted mean for the velocity. The Y-position of the green line shows the value of the weighted mean velocity.

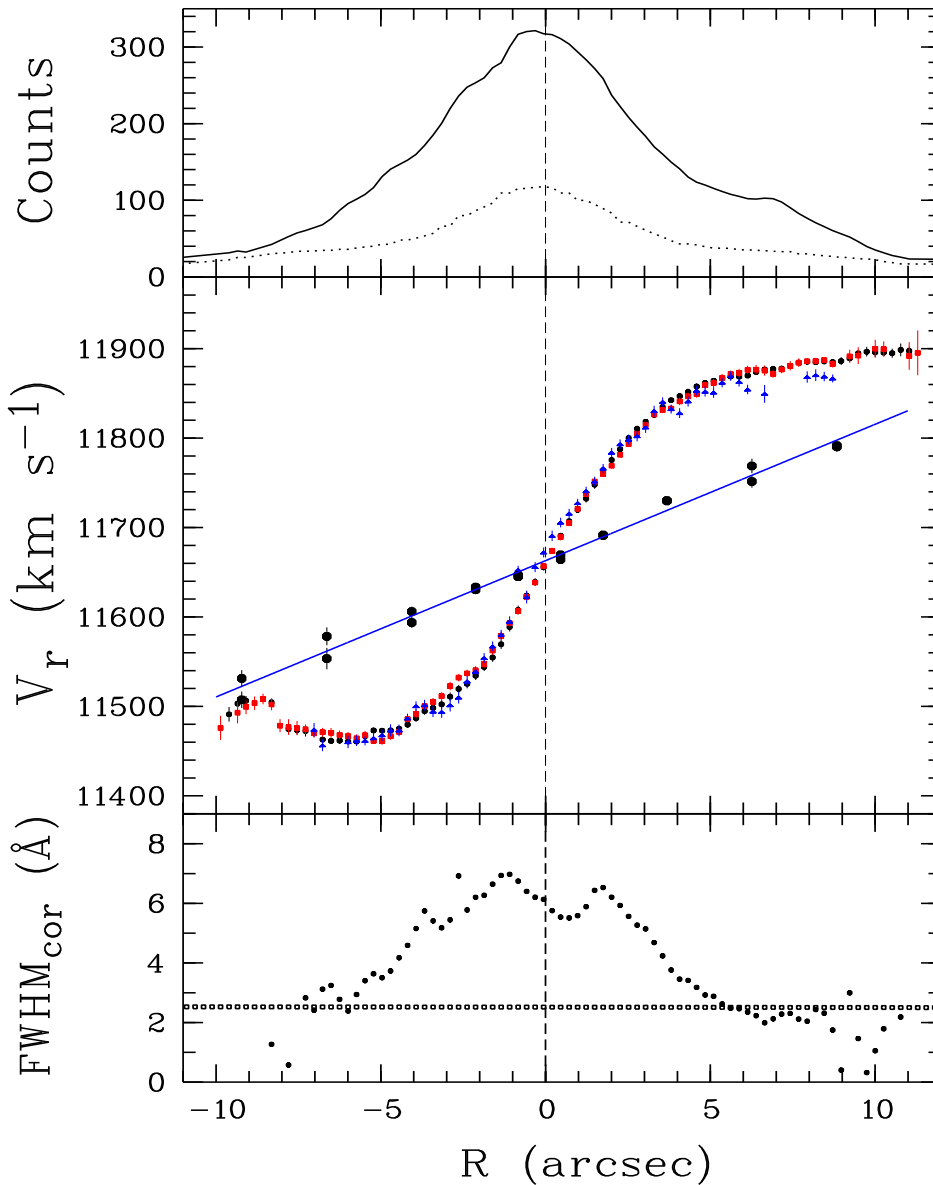


Figure 2: *Top panel:* The solid line shows the profile of the $H\alpha$ flux along the major axis, after the continuum subtraction. The dotted line shows the continuum intensity distribution along the slit and in the spectral region of the $H\alpha$ line. *Middle panel:* Radial velocity distribution along the major axis of AM 1934-563. The black squares, red squares and blue triangles represent measurements of the emission lines $H\alpha$, $[N\ II]\ \lambda 6583$ and $[S\ II]\ \lambda 6716$ respectively. The black filled circles show the stellar velocity distribution measured from the absorption doublet $Na\ I\ D\ \lambda\lambda 5890, 5896$. One σ error bars have been overplotted for all measurements. The solid blue line is the result of a linear fit to all measurements of the $Na\ I\ D$ lines. *Bottom panel:* The measured FWHM of the $H\alpha$ line, corrected for the intrinsic line width of the RSS. The FWHM of the reference night-sky line measured in each row is shown with open squares.

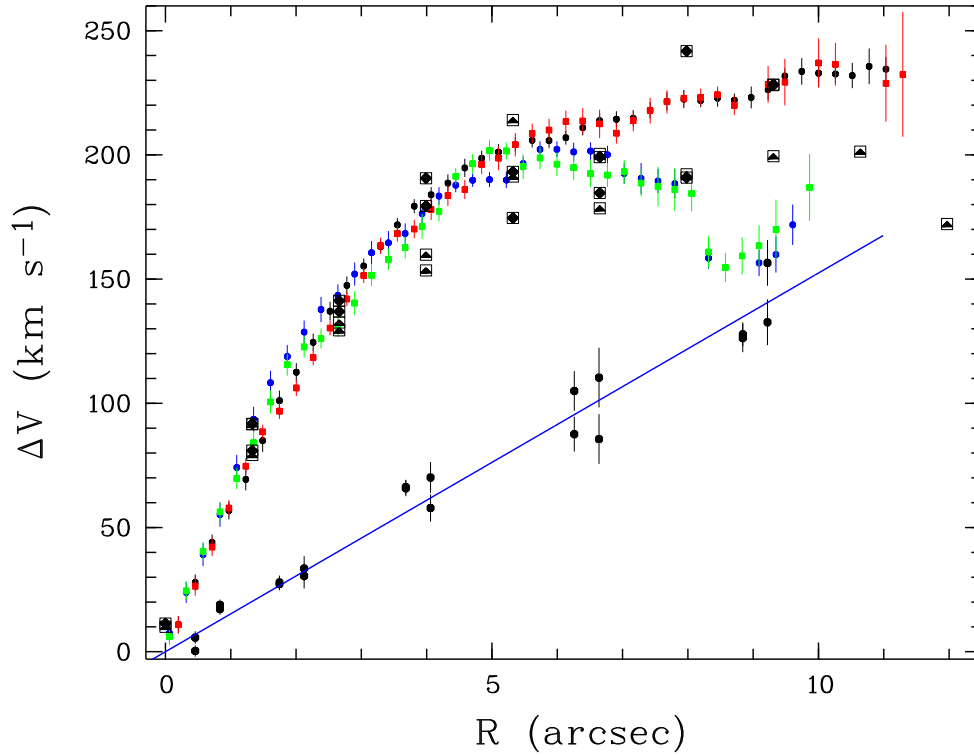


Figure 3: The galacto-centric velocity distributions along the major axis of AM 1934-563. The small black filled circles red squares are for the NW branch using the emission lines of $H\alpha$ and $[N II] \lambda 6583$ lines, respectively. The blue and green filled circles stand for the SE branch using the $H\alpha$ and $[N II] \lambda 6583$ lines. The larger filled black circles show the stellar velocity distribution measured from the absorption doublet $NaID \lambda\lambda 5890, 5896$. The solid blue line is the result of a linear fit to all measurements for the $NaID$ lines. Big black filled lozenges and triangles inside squares represent the Reshetnikov et al. (2006) data for $H\alpha$ and $[N II] \lambda 6583$, respectively. These values have not been corrected back for cosmological stretch.



3 Results

3.1 Data with grating VPH1800

3.1.1 Data for the dust-lane polar-ring galaxy AM 1934-563

The long-slit spectroscopic observations of the dust-lane polar-ring galaxy AM 1934-563 were obtained with the Southern African Large Telescope (SALT) during its performance-verification phase in 2006 to test the accuracy of velocity measurements with RSS and were published by Brosch et al. (2007). The spectra obtained on the nights of September 2006 were taken during stable weather conditions with seeing ~ 1.5 arcsec. They were done with grating GR1800 and cover the range from $\sim 6050\text{\AA}$ to $\sim 7300\text{\AA}$ with a spectral resolution of $0.4 \text{ \AA pixel}^{-1}$ or 2.4 \AA FWHM . All data were taken with a 1.5 arcsec wide slit.

The rotation curve of AM 1934-563 along the major axis is shown in Figures 2 and 3. Figure 2 shows the velocity-position plot and Figure 3 shows the galacto-centric velocity-distance plot. In general, the emission-line rotation curve derived in Brosch et al. (2007) corresponds with the one shown in Figure 5 of Reshetnikov et al. (2006), except that SALT data are better sampled, have a higher signal-to-noise, and the rotation curves derived from the different emission lines practically coincide, as can be estimated from the formal 1σ error bars plotted in the figures and from the scatter of the individual points. Figure 3 shows also a comparison of SALT measurements with those of Reshetnikov et al. (2006).

In deriving the rotation curves shown in Figures 2 and 3 Brosch et al. (2007) it was found that the systemic radial velocity of AM 1934-563 was $11663 \pm 3 \text{ km sec}^{-1}$, formally higher by some 14 km sec^{-1} than the value given by Reshetnikov et al. (2006) in their Table 3, but consistent with their value within the quoted uncertainties.

Brosch et al. (2007) could also derive the velocity dispersion of the $H\alpha$ line along the major axis; this is shown in the bottom panel of Figure 2. The dispersion is shown as the FWHM of the line after correcting for the intrinsic spectrometer line width. The corrected $H\alpha$ line FWHM = $5\text{--}7 \text{ \AA}$ found for the central part (± 3 arcsec) of AM 1934-563 indicates internal motions of $200\text{--}300 \text{ km s}^{-1}$.

3.1.2 Data for the dwarf irregular galaxy IC 4662

The long-slit spectroscopic observations of the dwarf irregular galaxy IC 4662 were obtained with SALT in 2006, to test the accuracy of velocity measurements and emission lines ratios. A paper on this topic is in preparation (Kniazev et al., 2013). VPH grating GR1800 with dispersion of $\sim 0.41 \text{ \AA pixel}^{-1}$ and spectral resolution FWHM of $2\text{--}2.5 \text{ \AA}$ was used to obtain the line-of sight velocity distribution along the slit.

These data can be compared with $H\alpha$ and HI velocity distributions published for IC 4662 in (van Eymeren et al., 2010). Such a comparison is shown in Figure 4, where the top shows the final $H\alpha$ velocity distribution for PA = 50 degrees based on SALT data. The bottom figure shows the part of Figure 12 from van Eymeren et al. (2010) with plotted $H\alpha$ velocity distribution for about the same position angle obtained with ESO NTT with similar reciprocal

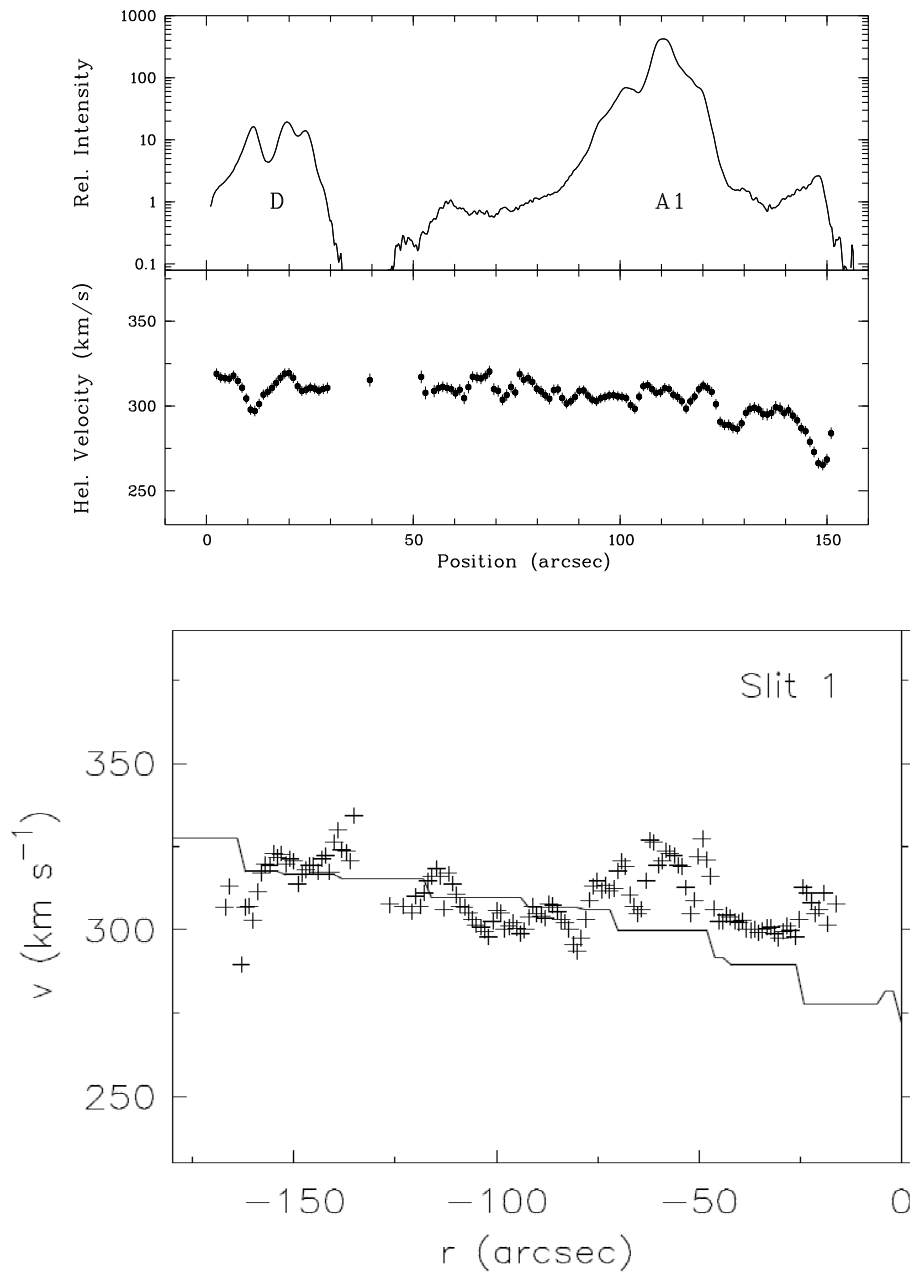


Figure 4: *Top figure*: RSS data. The solid line in the upper panel shows the profile of the H α flux along the major axis, after the continuum subtraction. Radial velocity distribution along the major axis of IC 4662 is shown in the bottom panel with 1σ errors for each point. *Bottom figure*: Radial velocity distribution along the major axis of IC 4662 from Figure 12 of van Eymeren et al. (2010): Optical data are shown with symbols '+'. HI velocities are shown with a solid line.



dispersion $\sim 0.41 \text{ \AA pixel}^{-1}$. The HI velocities obtained from the high-resolution velocity map, taken with the Australia Telescope Compact Array (ATCA), are also shown.

The result of comparison shows that SALT and NTT data show very similar velocity distributions with differences no more than 10 km s^{-1} . Possibly larger differences exist in the strongest HII region A1, due to small errors in the slit positions. The result of comparison with the HI velocities distribution are also consistent. For both comparisons we can conclude that differences do not exceed internal errors of SALT 2D wavelength calibrations ($\sim 10 \text{ km s}^{-1}$).

3.2 Data with grating VPH900

3.2.1 Data for lenticular galaxies

Data for some lenticular galaxies were observed during performance-verification phase in 2011. Data for four galaxies observed with grating GR900 were reduced (see Table 1). An example of velocity distributions for the emission $H\alpha$ is shown in Figure 1. The results of the weighted mean velocities with their errors are shown in Table 2. Calculated velocities were compared with values from NED, which are also shown in Table 2. The weighted mean difference $\Delta V(\text{SALT}-\text{NED})$ is $2.9 \pm 4.8 \text{ km s}^{-1}$.

Table 2: Velocities comparison for some lenticular galaxies

Galaxy Name	SALT (km/s)	NED (km/s)	Comment
NGC 216	1550 ± 5	1544 ± 6	HIPASS
NGC 2328	1186 ± 4	1183 ± 13	21-cm
IC 5267	1713 ± 5	1712 ± 5	21-cm
NGC 6893	3050 ± 9	3056 ± 26	optical

3.2.2 Velocities for PNe in the CMa region

Data for some Planetary Nebulae (PNe) in the CMa region were observed during 2012. All data were taken with grating GR900 (see Table 1). The data were reduced and velocity distributions for the emission $H\alpha$ were calculated. The results of the weighted mean velocities with their errors are shown in Table 3. Calculated velocities were compared with values from Schneider et al. (1983) and Durand, Acker & Zijlstra (1998), which are also shown in Table 3.

The comparison between SALT and other measurements is shown in Figure 5, where each measurement is shown with 1σ error (red for SALT and green for others) and the black line shows the equality relation. Points located far from the equality line have the largest errors from Schneider et al. (1983); Durand, Acker & Zijlstra (1998). The weighted mean difference $\Delta V(\text{SALT}-\text{Other})$ is $0.4 \pm 1.2 \text{ km s}^{-1}$. The weighted r.m.s. for $\Delta V(\text{SALT}-\text{Other})$ is 4.0 km s^{-1} .

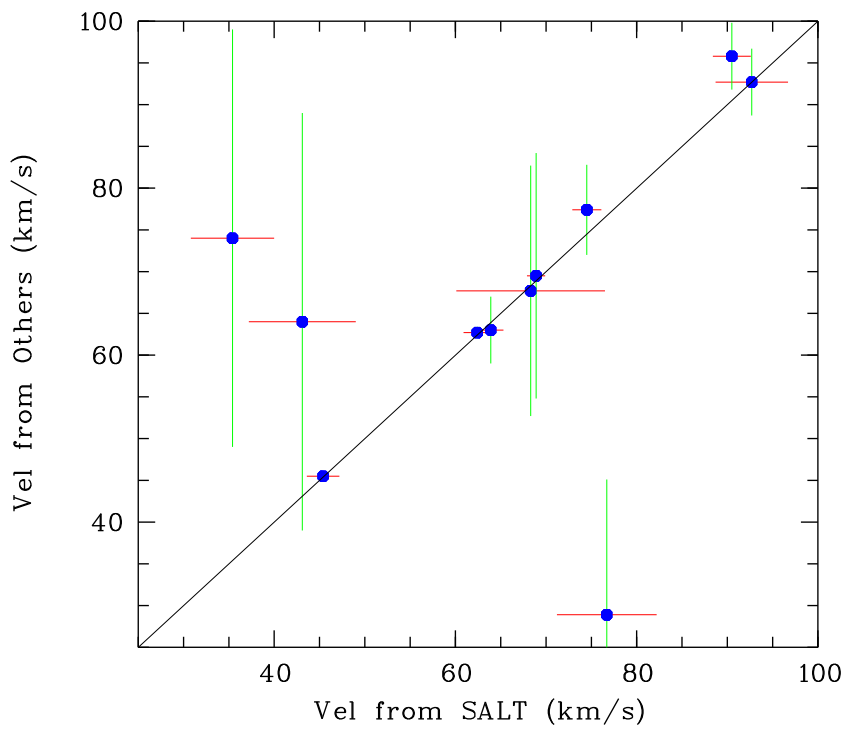


Figure 5: The comparison between SALT and other measurements. Each point is shown with 1σ error. Errors for SALT data are shown with red colour and errors from Schneider et al. (1983); Durand, Acker & Zijlstra (1998) are shown with green colour. Black lines shows the equality relation.



Table 3: Velocities comparison for PNe in the CMa region

PN Name	SALT (km/s)	Others (km/s)
065512-290727	92.7±4.0	92.7±4.0
070249-313529	68.9±1.0	69.5±14.7
071116-195102	76.7±5.5	28.9±16.2
071449-275023	68.3±8.2	67.7±15.0
071921-214355	90.5±2.1	95.8±4.0
072115-180834	45.4±1.8	45.5±0.3
072756-201322	74.5±1.6	77.4±5.4
074154-181229	62.4±1.5	62.7±0.7
074726-272006	63.9±1.4	63.0±4.0
075511-233812	35.4±4.6	74.0±25.0
080228-274155	43.1±5.9	64.0±25.0

4 Conclusions

In this report I studied the external consistency for velocities data based on emission lines in the spectra obtained with gratings GR900 and GR1800 of RSS/SALT. All analysed data were observed in the standard manner – one or more science frames 600–900 sec each and a reference arc spectrum was taken immediately after that.

- All analysed data show that with RSS data user can routinely reach an accuracy of $\sim 10 \text{ km s}^{-1}$ with grating GR900 and $\sim 5 \text{ km s}^{-1}$ with grating GR1800.
- No systematic velocity shifts were detected.

References

- Brosch N., et al., 2007, MNRAS, 382, 1809
Crawford S.M. et al., 2010, SPIE, 7737
Durand S., Acker A., Zijlstra A. 1998, A&AS, 132, 13
Kniazhev A.Y. et al., 2008, MNRAS, 388, 1667
Kniazhev A.Y. et al., 2013, MNRAS, in preparation
Reshetnikov, V., Bournaud, F., Combes, F., Faúndez-Abans, M., and de Oliveira-Abans, M., 2006, A&A, 446, 447
Schneider, S. E.; Terzian, Y.; Purgathofer, A.; Perinotto, M. 1983, ApJS, 52, 399
van Eymeren J., Koribalski B.S., Lopez-Sanchez A.R., Dettmar R.-J., Bomans D.J., 2010, MNRAS, 407, 113
Zasov A., Kniazhev A., Pustilnik S., Pramsky A., Burenkov A., Martin J.-M., 2000, A&AS, 144, 429